

Development of Novel ^{123}I -Labeled Pyridyl Benzofuran Derivatives for SPECT Imaging of β -Amyloid Plaques in Alzheimer's Disease

Masahiro Ono^{1*}, Yan Cheng¹, Hiroyuki Kimura¹, Hiroyuki Watanabe¹, Kenji Matsumura¹, Masashi Yoshimura¹, Shimpei Iikuni¹, Yoko Okamoto², Masafumi Ihara², Ryosuke Takahashi², Hideo Saji¹

1 Department of Patho-Functional Bioanalysis, Graduate School of Pharmaceutical Sciences, Kyoto University, Kyoto, Japan, **2** Department of Neuroscience, Graduate School of Medicine, Kyoto University, Kyoto, Japan

Abstract

Imaging of β -amyloid ($\text{A}\beta$) plaques in the brain may facilitate the diagnosis of cerebral β -amyloidosis, risk prediction of Alzheimer's disease (AD), and effectiveness of anti-amyloid therapies. The purpose of this study was to evaluate novel ^{123}I -labeled pyridyl benzofuran derivatives as SPECT probes for $\text{A}\beta$ imaging. The formation of a pyridyl benzofuran backbone was accomplished by Suzuki coupling. [$^{123}\text{I}/^{125}\text{I}$]-labeled pyridyl benzofuran derivatives were readily prepared by an iododestannylation reaction. In vitro $\text{A}\beta$ binding assays were carried out using $\text{A}\beta(1-42)$ aggregates and postmortem human brain sections. Biodistribution experiments were conducted in normal mice at 2, 10, 30, and 60 min postinjection. $\text{A}\beta$ labeling in vivo was evaluated by small-animal SPECT/CT in Tg2576 transgenic mice injected with [^{123}I]8. Ex vivo autoradiography of the brain sections was performed after SPECT/CT. Iodinated pyridyl benzofuran derivatives showed excellent affinity for $\text{A}\beta(1-42)$ aggregates (2.4 to 10.3 nM) and intensely labeled $\text{A}\beta$ plaques in autoradiographs of postmortem AD brain sections. In biodistribution experiments using normal mice, all these derivatives displayed high initial uptake (4.03–5.49% ID/g at 10 min). [^{125}I]8 displayed the quickest clearance from the brain (1.30% ID/g at 60 min). SPECT/CT with [^{123}I]8 revealed higher uptake of radioactivity in the Tg2576 mouse brain than the wild-type mouse brain. Ex vivo autoradiography showed in vivo binding of [^{123}I]8 to $\text{A}\beta$ plaques in the Tg2576 mouse brain. These combined results warrant further investigation of [^{123}I]8 as a SPECT imaging agent for visualizing $\text{A}\beta$ plaques in the AD brain.

Citation: Ono M, Cheng Y, Kimura H, Watanabe H, Matsumura K, et al. (2013) Development of Novel ^{123}I -Labeled Pyridyl Benzofuran Derivatives for SPECT Imaging of β -Amyloid Plaques in Alzheimer's Disease. PLoS ONE 8(9): e74104. doi:10.1371/journal.pone.0074104

Editor: Xiaoyuan Chen, NIH, United States of America

Received: February 18, 2013; **Accepted:** July 29, 2013; **Published:** September 13, 2013

Copyright: © 2013 Ono et al. This is an open-access article distributed under the terms of the Creative Commons Attribution License, which permits unrestricted use, distribution, and reproduction in any medium, provided the original author and source are credited.

Funding: This research is granted by the Japan Society for the Promotion of Science (JSPS) through the "Funding Program for Next Generation World-Leading Researchers (NEXT Program)," initiated by the Council for Science and Technology Policy (CSTP). The funders had no role in study design, data collection and analysis, decision to publish, or preparation of the manuscript.

Competing Interests: The authors have declared that no competing interests exist.

* E-mail: ono@pharm.kyoto-u.ac.jp

These authors contributed equally to this work.

Introduction

Alzheimer's disease (AD) is a leading cause of dementia with symptoms that include cognitive decline, irreversible memory loss, disorientation, language impairment, and an inability to carry out normal daily functions. Currently, it is difficult for clinicians to differentiate between the cognitive decline associated with normal aging and that associated with AD. A definitive diagnosis of AD can only be established by postmortem histopathological examination. Postmortem brains of AD patients reveal neuropathological features including senile plaques (SPs) and neurofibrillary tangles (NFTs), which contain β -amyloid ($\text{A}\beta$) peptides and highly phosphorylated tau proteins, respectively [1,2]. In particular, the formation of $\text{A}\beta$ plaques in the brain has been proposed to play an important role in the pathogenesis of AD for several reasons: 1) $\text{A}\beta$ deposits years before the onset of AD and can precede NFT formation; 2) mutation in the APP gene leads to some forms of early onset familial AD; and 3) $\text{A}\beta$ is toxic to cultured neurons [3–5]. The availability of probes for imaging $\text{A}\beta$ in vivo with

noninvasive techniques such as positron emission tomography (PET) and single photon emission computed tomography (SPECT) would enable the presymptomatic diagnosis of cerebral β -amyloidosis, risk prediction of AD, and monitoring of the effectiveness of anti-amyloid therapies [4]. Thus, great efforts have been made to develop radiotracers that bind to $\text{A}\beta$ plaques in vivo [6–10].

Over the past few years, initial studies with PET have suggested that many radiotracers show affinity for $\text{A}\beta$ in vivo, several of which have been subjected to clinical trials, including [^{11}C]2-(4'-(methylaminophenyl)-6-hydroxybenzothiazole (PIB) [11,12], 2-(3-[^{18}F]-fluoro-4-methylaminophenyl)benzothiazol-6-ol (GE-067, flutemetamol) [13], (*E*)-4-(*N*-methylamino)-4'-(2-(2-[^{18}F]-fluoroethoxy)ethoxy)ethoxy)-stilbene (BAY94-9172, florbetaben) [14], (*E*)-4-(2-(6-(2-(2-[^{18}F]-fluoroethoxy)ethoxy)ethoxy)pyridin-3-yl)vinyl)-*N*-methylaniline (AV-45, florbetapir) [15–17], and 2-(2-[^{18}F]-fluoro-6-(methylamino)pyridin-3-yl)benzofuran-5-ol (AZD4694) [18]. AV-45 has recently been approved by the US Food and Drug Administration (FDA) for the clinical diagnosis of AD by

exclusion. These PET probes differ in their uptake and retention in the brain between AD patients and controls, suggesting the feasibility of visualizing A β plaques in AD brains. However, the short half-lives of C-11 (20 min) and F-18 (110 min) mean they must be prepared from a cyclotron on-site, and the number of facilities with PET cameras is limited. PET is similar to SPECT in its use of radiolabeled probes and detection of γ rays. In contrast with PET, however, the probes used in SPECT emit γ radiation that is measured directly, whereas PET probes emit positrons that annihilate electrons, causing two γ photons to be emitted in opposite directions. A PET scanner detects these emissions coincidentally to provide higher resolution images than SPECT. Conversely, SPECT scans are significantly less expensive than PET scans because they are able to utilize longer-lived more easily-obtained radioisotopes such as ^{99m}Tc (6 h) or ^{123}I (13 h) than PET. Then, since SPECT would be more appropriate than PET for routine diagnostic use, there is a need to develop more useful A β imaging agents for SPECT to diagnose preclinical AD patients, the numbers of which are expected to increase as populations continue to age rapidly all over the world.

Although several radioiodinated or ^{99m}Tc -labeled ligands for A β plaques have been reported, unfavorable pharmacokinetics in vivo such as low uptake into the brain and slow washout have prevented clinical studies [9]. [^{123}I]6-iodo-2-(4'-dimethylamino)-phenyl-imidazo[1,2-*a*]pyridine (IMPY) is the first SPECT imaging agent to be tested in humans [19–21]. Although [^{123}I]IMPY showed excellent properties as a A β imaging probe in preclinical studies, the preliminary clinical data displayed a low signal-to noise ratio, making it difficult to distinguish AD patients, possibly due to high lipophilicity and low stability in vivo [21]. There is therefore no SPECT imaging probe useful for the clinical diagnosis of AD.

Recently, we have reported the utility of a series of novel ^{18}F -labeled benzofuran derivatives for PET imaging of A β plaques in the brain [22–24]. One of the derivatives, [^{18}F]FPYBF-2, showed selective affinity for A β plaques and good pharmacokinetics in the brain, and is currently in preparation for clinical trials [24]. More recently, we have reported the development of ^{99m}Tc -labeled pyridyl benzofuran derivatives as SPECT probes targeting A β plaques [25]. Although the ^{99m}Tc derivative successfully labeled some A β plaques in ex vivo autoradiographic studies, there were many A β plaques that could not be labeled, indicating that further improvement of the binding affinity to A β aggregates and brain uptake is necessary. This may be attributable to the bulkiness of the ^{99m}Tc -complex introduced in the pyridyl benzofuran scaffold. To develop more promising radiotracers for SPECT-based imaging of A β plaques, we planned to change ^{99m}Tc to ^{123}I as the radioisotope introduced in the pyridyl benzofuran scaffold.

In the present study, we designed and synthesized a novel series of iodinated pyridyl benzofuran derivatives and evaluated their biological potential as SPECT probes for visualizing A β plaques in vivo. Herein, we report the in vitro and in vivo evaluation and SPECT/CT imaging of these derivatives.

Materials and Methods

General

All reagents used in syntheses were purchased from Nacalai Tesque, Inc., Wako Pure Chemical Industries, Ltd., or Aldrich Co., and were used without further purification. ^1H -NMR spectra were obtained at 400 MHz on JEOL JNM-AL400 NMR spectrometers at room temperature with tetramethylsilane (TMS) as an internal standard. Chemical shifts are reported as δ values (parts per million) relative to the internal TMS. Coupling constants are reported in Hertz. Multiplicity is defined by s

Table 1. Inhibition Constants for the Binding of [^{125}I]IMPY to A β (1–42) Aggregates.

Compound	K_i (nM) ^a
7	10.3 ± 1.48
8	2.94 ± 0.22
9	2.36 ± 0.53
IMPY ^b	10.5 ± 1.05
PIB ^b	9.00 ± 1.31

^aValues are the means \pm standard errors of the mean of three independent determinations.

^bData from ref. [24].

doi:10.1371/journal.pone.0074104.t001

(singlet), d (doublet), t (triplet), and m (multiplet). Mass spectra were acquired with a Shimadzu GC-MS-QP2010 Plus (ESI). Fluorescence observations were made using a microscope (Nikon Eclipse 80i) with a BV-2A filter set (excitation, 400–440 nm; dichroic mirror, 455 nm; long pass filter, 470 nm). Reversed-phase HPLC (RP-HPLC) and analyses of radiolabeled and nonradioactive analogs were performed with a Shimadzu system (a LC-10AT pump with a SPD-10A UV detector, $\lambda = 254$ nm) and a Cosmosil C18 column (Nacalai Tesque, 5C₁₈-AR-II, 4.6 mm \times 150 mm) using a mobile phase (acetonitrile : water = 7 : 3) delivered at a flow rate of 1.0 mL/min. ddY mice (5 weeks, 22–25 g, male) were purchased from Shimizu Laboratory Supplies Co. Ltd. Tg2576 transgenic mice and wild-type mice were purchased from Taconic Farms, Inc. Small-animal μ SPECT/CT (FX3300; Gamma Medica-Ideas, Sherbrooke, Canada) was conducted in the Radioisotope Research Center, Kyoto University. All animal studies were conducted in accordance with our institutional guidelines and approved by Kyoto University Animal Care Committee.

Chemistry

5-(5-Bromobenzofuran-2-yl)pyridin-2-amine (1). A solution of 5-bromobenzofuran-2-boronic acid (722 mg, 3.0 mmol), 2-amino-5-iodopyridine (660 mg, 3.0 mmol), and Pd(Ph₃P)₄ (366 mg, 0.3 mmol) in 2 M Na₂CO₃ (aq.)/dioxane (150 mL, 1:1) was stirred under reflux overnight. The mixture was allowed to cool to room temperature, and 1 M NaOH (20 mL) was added. After extraction with ethyl acetate, the organic phase was dried over Na₂SO₄ and filtered. The filtrate was concentrated and the residue was purified by silica gel chromatography (hexane : ethyl acetate = 1 : 6) to give 273 mg of **1** (31.5%). ^1H NMR (400 MHz, CDCl₃): δ 4.66 (s, 2H), 6.57 (d, 1H, $J = 8.4$ Hz), 6.79 (s, 1H), 7.32 (d, 1H, $J = 2.4$ Hz), 7.33 (d, 1H, $J = 2.0$ Hz), 7.66 (d, 1H, $J = 1.6$ Hz), 7.86 (dd, 1H, $J_1 = 8.8$ Hz, $J_2 = 2.4$ Hz), 8.58 (d, 1H, $J = 2.4$ Hz). MS: m/z 290 (M⁺+H).

5-(5-Bromobenzofuran-2-yl)-*N*-methylpyridin-2-amine (2). The same reaction as described above to prepare **1** was employed, and **2** was obtained in 38.0% yield from 5-bromobenzofuran-2-boronic acid and 5-iodo-*N*-methylpyridin-2-amine. ^1H NMR (400 MHz, CDCl₃): δ 2.98 (d, 3H, $J = 5.2$ Hz), 4.80 (s, 1H), 6.45 (d, 1H, $J = 8.8$ Hz), 6.75 (s, 1H), 7.32 (d, 1H, $J = 7.2$ Hz), 7.52 (d, 1H, $J = 8.4$ Hz), 7.64 (d, 1H, $J = 2.0$ Hz), 7.87 (dd, 1H, $J_1 = 8.8$ Hz, $J_2 = 2.4$ Hz), 8.60 (d, 1H, $J = 2.8$ Hz). MS: m/z 304 (M⁺+H).

5-(5-Bromobenzofuran-2-yl)-*N,N*-dimethylpyridin-2-amine (3). The same reaction as described above to prepare **1** was employed, and **3** was obtained in 37.2% yield from 5-

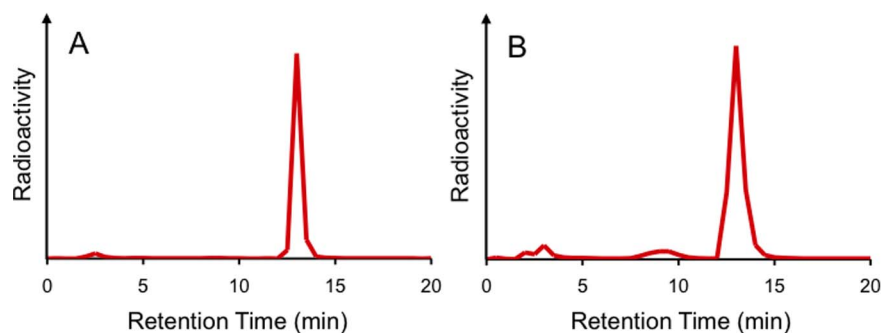


Figure 1. RP-HPLC profiles of $[^{125}\text{I}]\mathbf{8}$ in mouse plasma before (A) and after incubation for 1 h (B) at 37°C .
doi:10.1371/journal.pone.0074104.g001

bromobenzofuran-2-boronic acid and 5-iodo-*N,N*-dimethylpyridin-2-amine. ^1H NMR (400 MHz, CDCl_3): δ 3.14 (s, 6H), 6.55 (d, 1H, $J=8.8$ Hz), 6.71 (s, 1H), 7.17 (dd, 1H, $J_1=8.8$ Hz, $J_2=2.4$ Hz), 7.32 (d, 1H, $J=2.4$ Hz), 7.53 (d, 1H, $J=8.8$ Hz), 7.88 (dd, 1H, $J_1=8.8$ Hz, $J_2=2.4$ Hz), 8.65 (d, 1H, $J=2.4$ Hz). MS: m/z 318 (M^+H).

5-(5-(Tributylstannyl)benzofuran-2-yl)pyridin-2-amine (4). A mixture of **1** (273 mg, 0.95 mmol), bis(tributyltin) (0.8 mL), and $(\text{Ph}_3\text{P})_4\text{Pd}$ (100 mg) in a mixed solvent (40 mL, 3:1 dioxane/triethylamine mixture) was stirred at 90°C overnight. After extraction with ethyl acetate, the organic phase was dried over Na_2SO_4 and filtered. The filtrate was concentrated and the residue was purified by silica gel chromatography (hexane : ethyl acetate = 1: 1) to give 115.6 mg of **4** (24.6%). ^1H NMR (400 MHz, CDCl_3): δ 0.87–0.91 (m, 9H), 1.06–1.10 (m, 6H), 1.32–1.39 (m, 6H), 1.54–1.62 (m, 6H), 4.75 (s, 2H), 6.54 (d, 1H, $J=8.0$ Hz), 6.82 (s, 1H), 7.31 (d, 1H, $J=8.0$ Hz), 7.47 (d, 1H, $J=8.4$ Hz), 7.63 (s, 1H), 7.85 (dd, 1H, $J_1=8.4$ Hz, $J_2=2.4$ Hz), 8.59 (d, 1H, $J=2.4$ Hz). HRMS (EI): m/z calcd for $\text{C}_{25}\text{H}_{36}\text{N}_2\text{OSn}$ (M^+) 500.1849, found 500.1847.

***N*-Methyl-5-(5-(tributylstannyl)benzofuran-2-yl)pyridin-2-amine (5).** The same reaction as described above to prepare **4** was used, and 27.7 mg of **5** was obtained in 28.4% yield from **2**. ^1H NMR (400 MHz, CDCl_3): δ 0.89 (t, 9H, $J=7.2$ Hz), 1.32–1.35 (m, 12H), 1.62–1.66 (m, 6H), 3.04 (s, 3H), 6.75 (d, 1H, $J=8.8$ Hz), 6.87 (s, 1H), 7.32 (d, 1H, $J=7.2$ Hz), 7.46 (d, 1H, $J=8.4$ Hz), 7.64 (d, 1H, $J=2.0$ Hz), 8.05 (d, 1H, $J=8.4$ Hz), 8.40 (d, 1H, $J=3.2$ Hz). HRMS (EI): m/z calcd for $\text{C}_{26}\text{H}_{38}\text{N}_2\text{OSn}$ (M^+) 514.2006, found 514.1998.

***N,N*-Dimethyl-5-(5-(tributylstannyl)benzofuran-2-yl)pyridin-2-amine (6).** The same reaction as described above

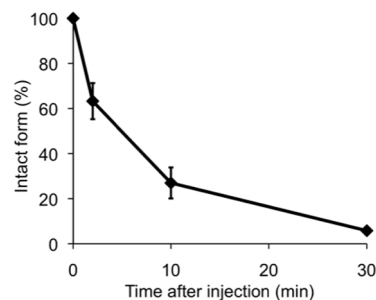


Figure 2. Percentage of the intact form in plasma after injection of $[^{125}\text{I}]\mathbf{8}$ into mice ($n=3$). Time-activity curves obtained from RP-HPLC of plasma samples at 2, 5, and 30 min after injection of $[^{125}\text{I}]\mathbf{8}$ into mice.
doi:10.1371/journal.pone.0074104.g002

to prepare **4** was used, and 88.9 mg of **6** was obtained in 25.1% yield from **3**. ^1H NMR (400 MHz, CDCl_3): δ 0.89 (t, 9H, $J=7.2$ Hz), 1.04–1.12 (m, 6H), 1.30–1.39 (m, 6H), 1.53–1.60 (m, 6H), 3.14 (s, 6H), 6.57 (d, 1H, $J=9.6$ Hz), 6.79 (s, 1H), 7.29 (d, 1H, $J=8.0$ Hz), 7.47 (d, 1H, $J=8.4$ Hz), 7.62 (s, 1H), 7.88 (dd, 1H, $J_1=9.6$ Hz, $J_2=2.4$ Hz), 8.67 (d, 1H, $J=2.4$ Hz). HRMS (EI): m/z calcd for $\text{C}_{27}\text{H}_{40}\text{N}_2\text{OSn}$ (M^+) 528.2162, found 528.2158.

5-(5-Iodobenzofuran-2-yl)pyridin-2-amine (7). To a solution of **4** (100 mg, 0.20 mmol) in CHCl_3 (5 mL) was added a solution of iodine in CHCl_3 (0.5 mL, 1 M) at room temperature. The mixture was stirred at room temperature for 10 min. A NaHSO_3 solution (3 mL, 5% in water) was added successively. The mixture was stirred for 5 min, and the organic phase was separated. The aqueous phase was extracted with CHCl_3 , and the combined organic phase was dried over Na_2SO_4 and filtered. The filtrate was concentrated and the residue was purified by silica gel chromatography (hexane : ethyl acetate = 1: 1) to give 34.9 mg of **7** (52.0%). ^1H NMR (400 MHz, CDCl_3): δ 4.66 (s, 2H), 6.57 (d, 1H, $J=8.4$ Hz), 6.77 (s, 1H), 7.27 (s, 1H), 7.51 (d, 1H, $J=8.0$ Hz), 7.84 (s, 1H), 7.85 (d, 1H, $J=2.4$ Hz), 8.58 (d, 1H, $J=2.4$ Hz). HRMS (EI): m/z calcd for $\text{C}_{13}\text{H}_9\text{IN}_2\text{O}$ (M^+) 335.9760, found 335.9752.

5-(5-Iodobenzofuran-2-yl)-*N*-methylpyridin-2-amine (8). The same reaction as described above to prepare **7** was used, and 50.2 mg of **8** was obtained in 65.1% yield from **5**. ^1H NMR (400 MHz, CDCl_3): δ 2.98 (d, 3H, $J=4.8$ Hz), 4.79 (s, 1H), 6.45 (d, 1H, $J=8.8$ Hz), 6.74 (s, 1H), 7.30 (s, 1H), 7.50 (d, 1H, $J=8.4$ Hz), 7.85 (s, 1H), 7.87 (d, 1H, $J=2.4$ Hz), 8.60 (d, 1H, $J=2.4$ Hz). HRMS (EI): m/z calcd for $\text{C}_{14}\text{H}_{11}\text{IN}_2\text{O}$ (M^+) 349.9916, found 349.9923.

5-(5-Iodobenzofuran-2-yl)-*N,N*-dimethylpyridin-2-amine (9). The same reaction as described above to prepare **7** was used, and 32.8 mg of **9** was obtained in 45.6% yield from **6**. ^1H NMR (400 MHz, CDCl_3): δ 3.14 (s, 6H), 6.55 (d, 1H, $J=8.8$ Hz), 6.70 (s, 1H), 7.25 (d, 1H, $J=4.0$ Hz), 7.47 (d, 1H, $J=8.4$ Hz), 7.82 (s, 1H), 7.84 (d, 1H, $J=2.4$ Hz), 8.65 (d, 1H, $J=2.4$ Hz). HRMS (EI): m/z calcd for $\text{C}_{15}\text{H}_{13}\text{IN}_2\text{O}$ (M^+) 364.0073, found 364.0065.

Radiosynthesis

Radioiodinated forms of pyridyl benzofuran derivatives were synthesized from the corresponding tributyltin derivatives. Briefly, to initiate the reaction, 100 μL H_2O_2 (3%) was added to a mixture of a tributyltin derivative (0.5 mg/100 μL of EtOH), 7.4 MBq of $[^{123}\text{I}]\text{NaI}$ or 0.74 MBq of $[^{125}\text{I}]\text{NaI}$, and 100 μL of 1 N HCl in a sealed vial. The reaction was allowed to proceed at room temperature for 10 min and was terminated by the addition of

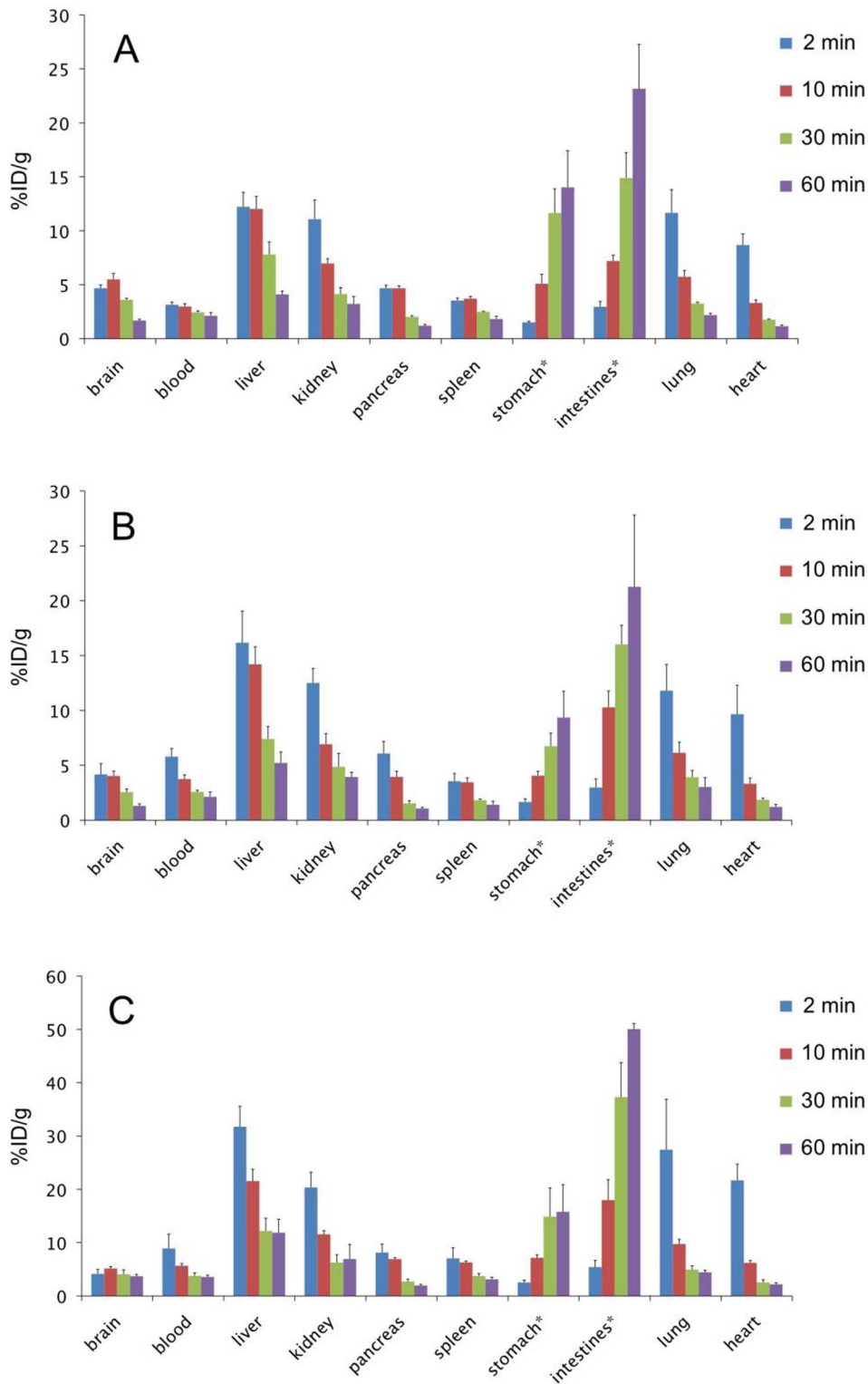


Figure 3. Biodistribution of radioactivity after injection of [¹²⁵I]7 (A), [¹²⁵I]8 (B), and [¹²⁵I]9 (C) in normal mice. Values are expressed as the mean %injected dose/g SD in groups of five animals for each time point. doi:10.1371/journal.pone.0074104.g003

NaHSO₃. After neutralization with sodium bicarbonate, the reaction mixture was extracted with ethyl acetate. The extract was dried by passing through an anhydrous Na₂SO₄ column and

blown dry with a stream of nitrogen gas. The radiolabeled ligands were purified by RP-HPLC.

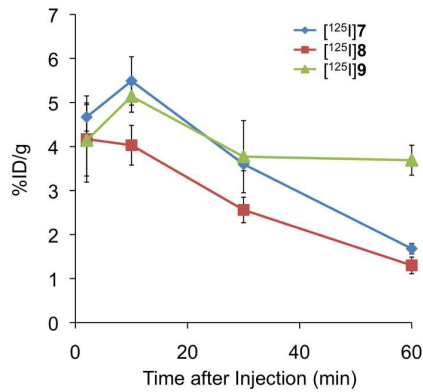


Figure 4. Comparison of brain uptake of three radioiodinated pyridyl benzofuran derivatives in normal mice.
doi:10.1371/journal.pone.0074104.g004

In Vitro Binding Assays Using Aggregated A β Peptides in Solution

A β (1–42) was purchased from the Peptide Institute (Osaka, Japan). Aggregation was carried out by gently dissolving the peptide (0.25 mg/mL) in a buffer solution (pH 7.4) containing 10 mM sodium phosphate and 1 mM EDTA. The solution was incubated at 37°C for 42 h with gentle and constant shaking. A mixture containing 50 μ L of iodinated pyridyl benzofuran derivative (0.008 pM–400 μ M in 10% EtOH), 50 μ L of [¹²⁵I]IMPY (0.02 nM), 50 μ L of A β (1–42) aggregates, and 850 μ L of 10% EtOH was incubated at room temperature for 3 h. The mixture was then filtered through Whatman GF/B filters using a Brandel M-24 cell harvester, and the radioactivity of the filters containing the bound ¹²⁵I ligand was measured in a γ counter. Values for the half-maximal inhibitory concentration (IC₅₀) were determined from displacement curves of three independent experiments using GraphPad Prism 5.0, and those for the inhibition constant (K_i) were calculated using the Cheng-Prusoff equation [26]: $K_i = IC_{50}/(1 + [L]/K_d)$, where [L] is the concentration of [¹²⁵I]IMPY used in the assay and K_d is the dissociation constant of IMPY (4.2 nM).

In Vitro Stability in Mouse Plasma

[¹²⁵I]8 (11 kBq, 10 μ L) was added to the mouse plasma (200 μ L), and the plasma samples were incubated at 37°C for 1 h. After incubation, plasma samples were mixed with equal volumes of acetonitrile followed by centrifugation at 4,500 rpm for 10 min to remove the denatured proteins. The supernatant was filtrated using a 0.45 μ m filter (Millipore; Billerica, MA, USA). Then, the filtrate was analyzed by RP-HPLC.

In Vivo Stability in Normal Mice

[¹²⁵I]8 (0.11 MBq, 100 μ L) was injected into the tail vein of ddY mice. The mice were sacrificed at 2, 10, and 30 min after the injection (male, n = 3 for each time point). The blood samples were centrifuged at 3,500 rpm for 10 min to separate plasma. Plasma samples were mixed with equal volumes of acetonitrile followed by centrifugation at 4,500 rpm for 10 min to remove the denatured proteins. The supernatant was filtrated using 0.45 μ m filter (Millipore; Billerica, MA, USA). Then, the filtrate was analyzed by RP-HPLC.

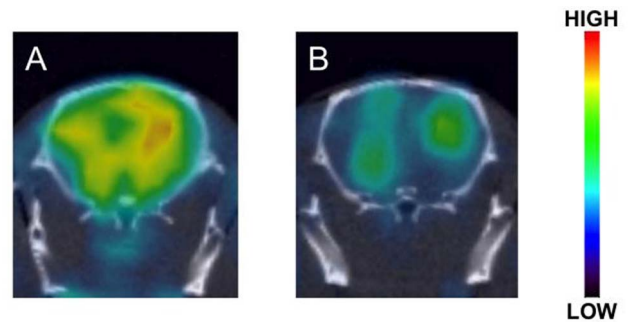


Figure 5. Brain SPECT images after injection of [¹²³I]8 into a Tg2576 mouse (A) and a wild-type mouse (B).
doi:10.1371/journal.pone.0074104.g005

Biodistribution in Normal Mice

While under anesthesia with 2% isoflurane, ddY mice were injected directly into a tail vein with 100 μ L of 10% EtOH containing ¹²⁵I-labeled pyridyl benzofuran derivatives (37 kBq). The mice (male, n = 5 for each time point) were sacrificed at 2, 10, 30, and 60 min postinjection. The organs of interest were removed and weighed, and radioactivity was measured with an automatic gamma counter (COBRAII; Packard). Percentage dose per organ was calculated by comparing the tissue counts to suitably diluted aliquots of the injected material. The %dose/g of samples was calculated by comparing the sample counts with the count of the diluted initial dose.

Small-Animal SPECT/CT

Dynamic SPECT scans were performed on a dedicated small-animal SPECT scanner (FX3300, Gamma Medica-Ideas). Tg2576 transgenic mice (28 months, female, n = 3) and wild-type mice (28 months, female, n = 3) were used as an Alzheimer's model and an age-matched control, respectively. Briefly, the animals were initially anesthetized with 2% isoflurane. When fully anesthetized, an animal was placed on the scanner bed, with a nose cone used to maintain anesthesia with 2% isoflurane throughout the experiment. [¹²³I]8 (20.5–26.5 MBq) in 10% aqueous EtOH solution

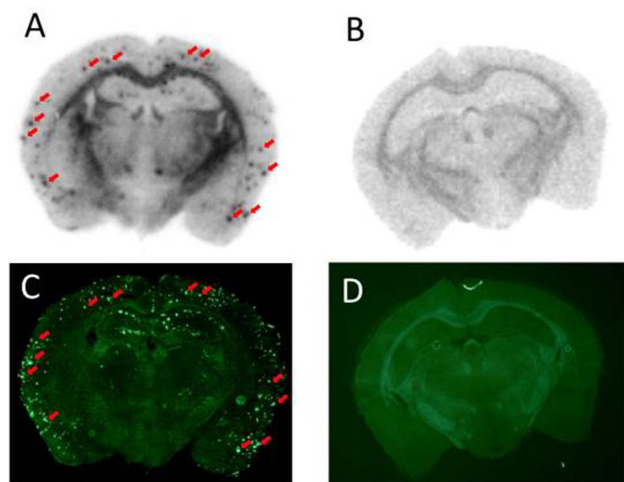


Figure 6. Ex vivo autoradiograms of brain sections after injection of [¹²³I]8 into a Tg2576 mouse (A) and a wild-type mouse (B). Fluorescent staining of the same brain section (A and B) with thioflavin S is shown in Figures C and D, respectively.
doi:10.1371/journal.pone.0074104.g006

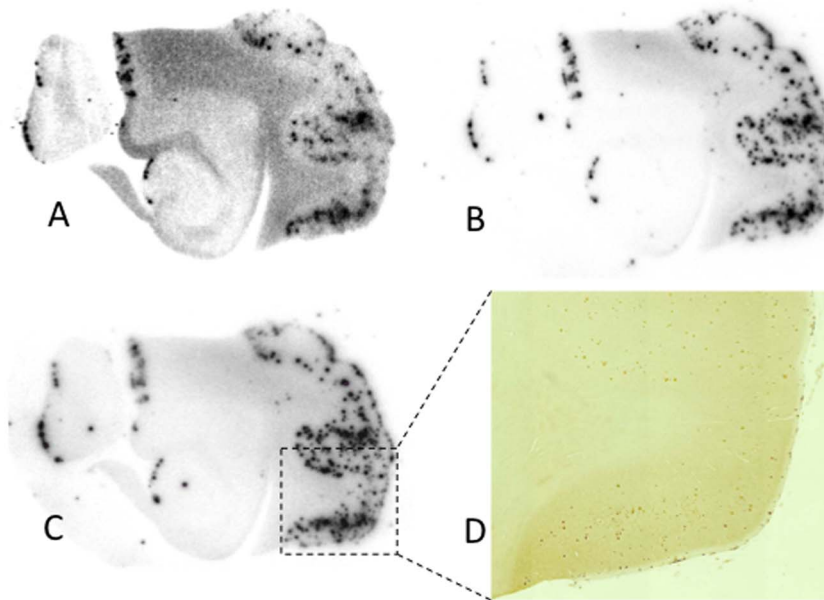


Figure 7. In vitro autoradiograms of sections of the AD brain labeled with $[^{125}\text{I}]7$ (A), $[^{125}\text{I}]8$ (B), and $[^{125}\text{I}]9$ (C). The A β plaques were confirmed by immunostaining (D).
doi:10.1371/journal.pone.0074104.g007

containing 0.1% Tween80 was injected into a tail vein. Dynamic data were acquired over a period of 60 min after the injection, followed by the acquisition of CT data over a period of 5 min. The SPECT data were reconstructed using a 3-dimensional ordered subsets expectation maximization (3D OSEM) algorithm (5 iteration, 8 subsets). The SPECT scan time was sorted by a 30-s time frame in each 1-min interval (total, 60 frames for a total scan time of 60 min). Overexpression of A β plaques was observed in the cortex of Tg2576 mice, but not in the cerebellum of Tg2576 mice or in any brain regions of wild-type mice. For statistical analyses, regions of interest (ROIs) were manually placed over the frontal cortex (FR) and cerebellum (CE) on the summed SPECT images of $[^{123}\text{I}]8$ in Tg2576 ($n = 3$) and wild-type ($n = 3$) mice. Identification of anatomical structures was guided by the stereotaxic mouse brain atlas. Differences in FR to CE ratio values between Tg2576 and wild-type mice were compared by unpaired t tests. The level of statistical significance was designated as $p < 0.05$.

Ex Vivo Autoradiography of Transgenic Mouse Brain

The animals were killed by decapitation after the SPECT analysis. Brains were immediately removed and frozen in a dry ice/hexane bath. Sections of 20 μm were cut and exposed to a BAS imaging plate (Fuji Film, Tokyo, Japan) overnight. Ex vivo film autoradiograms were thus obtained. After autoradiographic examination, the same sections were stained by thioflavin-S to confirm the presence of A β plaques. For staining with thioflavin-S, sections were immersed in a 0.125% thioflavin-S solution containing 50% EtOH for 5 min and washed in 50% EtOH. After drying, the sections were examined using a microscope (Eclipse 80i; Nikon) equipped with a B-2A filter set (excitation, 450–490 nm; dichroic mirror, 505 nm; long-pass filter, 520 nm).

In Vitro Autoradiography Using Human AD Brain Sections

Postmortem brain tissues from an anonymous autopsy-confirmed case of AD (93-year-old, female) were obtained from the Graduate School of Medicine, Kyoto University. Six-micrometer-

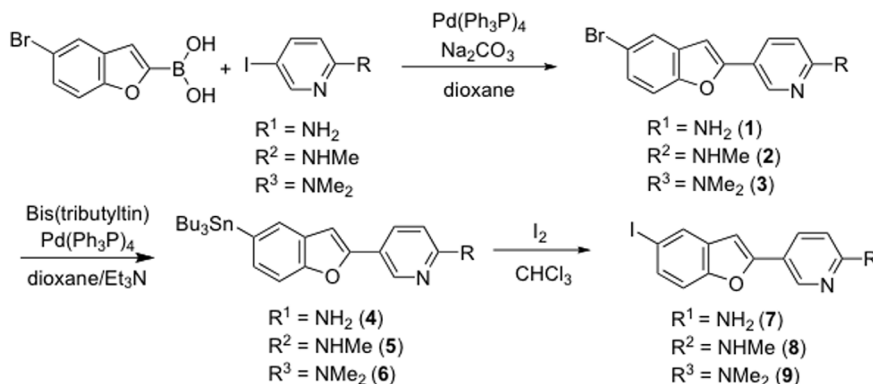


Figure 8. Scheme 1. Synthesis of iodinated pyridyl benzofuran derivatives.

doi:10.1371/journal.pone.0074104.g008

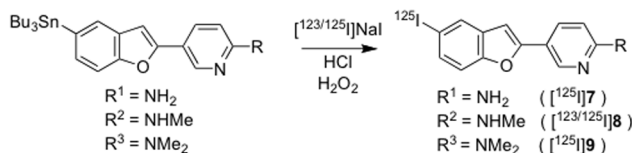


Figure 9. Scheme 2. Radiosynthesis of iodinated pyridyl benzofuran derivatives.

doi:10.1371/journal.pone.0074104.g009

thick serial sections of paraffin-embedded blocks were used for in vitro autoradiography. The sections were incubated with ¹²⁵I-labeled tracers (444 kBq/50 μ L) for 1 h at room temperature, then dipped in saturated Li₂CO₃ in 40% EtOH (two 2-min washes), washed with 40% EtOH (one 2-min wash), and rinsed with water for 30 s. After drying, the ¹²⁵I-labeled sections were exposed to a BAS imaging plate (Fuji Film) overnight. Autoradiographic images were obtained using a BAS5000 scanner system (Fuji Film). After autoradiographic examination, the same sections were immunostained using an amyloid β -protein immunohistochemical staining kit (Wako Pure Chemical Industries, Ltd.).

Results and Discussion

Chemistry

The key step in the formation of the pyridyl benzofuran backbone was accomplished with a Suzuki coupling reaction (Figure 8) [27]. Suzuki coupling afforded the desired compounds **1–3** in yields of 31.5, 38.0, and 37.2%, respectively. The bromo compounds (**1–3**) were then reacted with bis(tributyltin) using Pd(0) as the catalyst and the corresponding tributyltin derivatives (**4–6**) were obtained in yields of 24.6, 28.4, and 25.1%, respectively. These tributyltin derivatives were readily reacted with iodine in chloroform at room temperature to give iodo derivatives (**7–9**) in yields of 52.0, 65.1, and 45.6%, respectively. Furthermore, these tributyltin derivatives can be also used as the starting materials for radioiodination in the preparation of [¹²⁵I]**7**, [¹²³I/¹²⁵I]**8**, and [¹²⁵I]**9**. Novel radioiodinated pyridyl benzofuran derivatives were obtained by an iododestannylation reaction using hydrogen peroxide as the oxidant (Figure 9). It was anticipated that the no-carrier-added preparation would result in a final product bearing a theoretical specific activity similar to that of ¹²⁵I (81.4 TBq/mmol). The radiochemical identities of the radioiodinated ligands were verified by co-injection with the nonradioactive compounds by their HPLC profiles. [¹²⁵I]**7**, [¹²³I/¹²⁵I]**8**, and [¹²⁵I]**9** were obtained in 61–89% radiochemical yield with a radiochemical purity of >99% after purification by HPLC.

In Vitro Binding to A β (1–42) Aggregates

Initial screening of the affinity of iodinated pyridyl benzofuran derivatives was carried out with A β (1–42) aggregates, using [¹²⁵I]IMPY as the competing radioligand [22,28]. These derivatives inhibited the binding of [¹²⁵I]IMPY with *K_i* values in the nanomolar range (*K_i* = 2.4–10.3 nM), indicating that they had excellent affinity for A β (1–42) aggregates (Table 1). We have reported previously that ¹⁸F-labeled pyridyl benzofuran derivatives showed high affinity to A β (1–42) aggregates at *K_i* values from 2.4 to 3.9 nM, indicating that the pyridyl benzofuran core structure had considerable tolerance for structural modification with nucleophilic groups (NH₂, NHMe, NMe₂). The *K_i* values of IMPY and PIB as controls were 10.5 and 9.0 nM, respectively (Table 1). The affinity of iodinated pyridyl benzofuran derivatives was close to that of these known A β imaging tracers, suggesting

that these derivatives possess enough affinity to image A β aggregates in vivo.

In Vitro and in Vivo Stability in Mouse Plasma

We determined the in vitro and in vivo stability of [¹²⁵I]**8** in mouse plasma. When incubated [¹²⁵I]**8** in mouse plasma for 1 h, 77.4% of radioactivity derived from [¹²⁵I]**8** existed as an intact form (Figure 1), indicating that it should be relatively stable in mouse plasma. Conversely, as shown in Figure 2, when radioactivity was analyzed in mouse plasma by RP-HPLC after injection of [¹²⁵I]**8** into mice, we found conversion of [¹²⁵I]**8** to several different chemical forms. A percent of the intact form decreased with time and reached 20.7% at 30 min postinjection. This profile was comparable to that of [¹¹C]PIB in mice reported previously [29], suggesting that [^{123/125}I]**8** has sufficient in vivo stability for clinical trials. The difference in the stability of [¹²⁵I]**8** between in vitro and in vivo may be attributable to radiometabolites produced by the in vivo metabolism of [¹²⁵I]**8** in organs such as the liver and kidney.

In Vivo Biodistribution in Normal Mice

We determined the biodistribution of radioactivity after an intravenous injection of [¹²⁵I]**7**, [¹²⁵I]**8**, and [¹²⁵I]**9** in healthy mice (Figure 3). To define an acceptable PET or SPECT probe for imaging A β plaques in vivo, several common criteria have been set, such as: 1) high affinity for A β aggregates (*K_i* \leq 20 nM); 2) a sufficient amount of the agent entering the brain and non-specifically bound agent cleared from the brain; high initial uptake >0.5%ID/g at 2 min postinjection and quick washout from the brain (<30% of initial uptake remaining in the brain) [6,20] To directly compare the uptake and washout of three radioiodinated probes, a combined plot is presented in Figure 4. These ¹²⁵I-labeled derivatives penetrated the blood-brain barrier (BBB) soon after the injection (4.14–4.67%ID/g at 2 min postinjection), and the radioactivity cleared with time from the brain (1.30–3.69%ID/g at 60 min postinjection). [¹²⁵I]**8** peaked at 2 min postinjection, while [¹²⁵I]**7** and [¹²⁵I]**9** peaked at 10 min postinjection. Generally, the brain_{2min}/brain_{60 min} ratio has been used to compare the rate of washout from the brain. The brain_{2min}/brain_{60 min} ratios of [¹²⁵I]**7**, [¹²⁵I]**8**, and [¹²⁵I]**9** were 1.30, 3.21 and 1.12, respectively. The results in normal mice showed that the monomethylated pyridyl benzofuran derivative [¹²⁵I]**8**, the brain_{2min}/brain_{60 min} ratio of which was 3.21, exhibited not only high initial uptake in the brain but also quick washout from the brain over time, which are highly desirable properties for A β imaging probes (Figure 3). We have previously reported the development of radioiodinated phenylbenzofuran derivatives as SPECT imaging agent [30]. Although these derivatives displayed high uptake in normal mouse brain, the radioactivity washed out slowly, suggesting high non-specific binding in vivo. While the brain_{2min}/brain_{60 min} ratio of the radioiodinated phenylbenzofuran derivatives ranged from 0.47 to 0.65, the low brain_{2min}/brain_{60 min} ratio of the radioiodinated pyridyl benzofuran derivatives (1.12–3.21) indicated much better pharmacokinetics in the brain than the phenylbenzofuran derivatives. Furthermore, the brain_{2min}/brain_{60 min} ratio of [¹²⁵I]**8** (3.2) was close to that of [¹⁸F]AV-45 (3.8) [31], which is a PET imaging probe approved by the FDA, indicating that [¹²⁵I]**8** shows excellent pharmacokinetics in the brain sufficient to apply to clinical studies. We have reported previously that the brain_{2min}/brain_{60 min} ratio of ¹⁸F-labeled pyridyl benzofuran derivatives was 2.11–2.34, indicating that [¹²⁵I]**8** provided a better profile than ¹⁸F-labeled pyridyl benzofuran derivatives. The favorable in vivo pharmacokinetics of [¹²⁵I]**8** were achieved by substitution of the phenyl group with a

pyridyl group, which resulted in a less lipophilic compound. Since lipophilicity is an important factor affecting the uptake of a compound into the brain, it may be associated with the favorable pharmacokinetics of [125 I]**8** in the brain.

Radioactivity also distributed to several other organs, such as the liver, kidneys, stomach, and intestines, in addition to accumulating in the brain. The liver and kidneys showed initially high uptake and washout with time while the stomach and intestines showed an accumulation of radioactivity over time (Figure 3).

In Vivo Evaluation with Tg2576 mice

To prove the feasibility of A β imaging in vivo, SPECT/CT was performed in Tg2576 transgenic mice and wild-type mice after the intravenous injection of [123 I]**8**. Tg2576 transgenic mice have been widely used for in vitro and in vivo evaluations of A β imaging agents because of marked A β deposition in the brain [32]. In transverse SPECT images, a clear difference in the accumulation of radioactivity in the brain was observed between Tg2576 and wild-type mice (Figure 5). The mean FR/CE ratios were 1.34 ± 0.07 (average \pm SD) in Tg2576 mice ($n = 3$) and 1.01 ± 0.03 (average \pm SD) in wild-type mice ($n = 3$), the difference being significant ($p = 0.012$). Although further quantitative studies are necessary in the future, the statistical analyses appear to reflect the difference of radioactivity accumulation on the SPECT images between Tg2576 and wild-type mice.

To further characterize the specific binding of [123 I]**8** to A β plaques in brains, the brains were removed, frozen, and sectioned immediately after the SPECT/CT study for ex vivo autoradiography (Figure 6). Autoradiographic images showed extensive labeling of A β plaques in the brains of Tg2576 mice (Figure 6A) but not the wild-type control (Figure 6B). The labeling of A β plaques was confirmed by co-staining the same sections with thioflavin-S, a pathological dye commonly used for amyloid staining (Figure 6C). These results suggested that [123 I]**8** penetrated the intact BBB and bound to cerebral A β plaques strongly. Many A β -targeting tracers for SPECT reported previously did not penetrate the BBB or once they entered the brain, the nonspecific binding was so high that the agents could not provide a specific signal for A β plaques, despite their high binding affinity. To our knowledge, this is the first report that A β plaques in Tg2576 mouse brain were successfully imaged in vivo with a small-animal SPECT. These results also suggested the feasibility of in vivo A β imaging with [123 I]**8** in the brains of AD patients.

Autoradiography of Postmortem AD Brain Sections

To evaluate the binding of [125 I]**8** to A β plaques accumulated in human brains, in vitro autoradiography in postmortem AD brain

tissue sections was performed. A previous study reported the conformation of A β plaques in Tg2576 mice to be different from that in AD brains [33]. It is therefore very important to test the affinity for A β plaques in AD brains in addition to evaluations using Tg2576 mice. When the AD brain sections were incubated with [125 I]-labeled pyridyl benzofurans, autoradiographic images revealed excellent visualization of A β plaques with minimal background noise (Figure 7). No marked difference in the accumulation of radioactivity in AD brain sections was observed between [125 I]**8** and [125 I]**9** (Figure 7B and 7C). However, [125 I]**7** showed nonspecific binding in white matter in the brain, while it labeled A β plaques (Figure 7A). The spots of radioactivity derived from [125 I]**8** in the cortex were confirmed by immunostaining the same brain sections with A β antibody (Figure 7D). These results indicated that [123 I]**8** may be applied to the in vivo imaging of A β plaques in AD brains, and deserves further investigation as a promising SPECT imaging agent for the diagnosis of AD. Although a similar autoradiographic pattern was observed for both [125 I]**8** and [125 I]**9**, [125 I]**7** displayed nonspecific accumulation in white matter with the binding to A β plaques. In the binding assay, [125 I]**8** ($K_i = 2.94$ nM) and [125 I]**9** ($K_i = 2.36$ nM) showed higher affinity for A β aggregates than [125 I]**7** ($K_i = 10.3$ nM) (Table 1). Therefore, the difference in the autoradiographic study may be attributable to the affinity of the compounds.

Conclusion

On the basis of our previous results, we developed three novel iodinated pyridyl benzofuran ligands for imaging A β plaques in the brain. These ligands showed high affinity for A β aggregates in vitro and for A β plaques in sections of an autopsied AD brain. In biodistribution experiments using normal mice, [125 I]**8** displayed good uptake into and fast washout from the brain. In addition, a SPECT study and ex vivo autoradiograms of brain sections from Tg2576 mice after the injection of [123 I]**8** showed selective binding of A β plaques with little nonspecific binding. The results suggest that [123 I]**8** should be further investigated as a potentially useful SPECT imaging agent for cerebral A β plaques in the AD brain.

Author Contributions

Conceived and designed the experiments: MO MI RT HS. Performed the experiments: YC HK HW KM MY SI YO. Analyzed the data: YC HK HW KM. Contributed reagents/materials/analysis tools: MO YC HK YO MI. Wrote the paper: MO YC HW.

References

- Klunk WE (1998) Biological markers of Alzheimer's disease. *Neurobiol Aging* 19: 145–147.
- Selkoe DJ (2001) Alzheimer's disease: genes, proteins, and therapy. *Physiol Rev* 81: 741–766.
- Hardy J, Selkoe DJ (2002) The amyloid hypothesis of Alzheimer's disease: progress and problems on the road to therapeutics. *Science* 297: 353–356.
- Klunk WE (2011) Amyloid imaging as a biomarker for cerebral β -amyloidosis and risk prediction for Alzheimer dementia. *Neurobiol Aging* 32: S20–S36.
- Glennner GG, Wong CW (1984) Alzheimer's disease and Down's syndrome: sharing of a unique cerebrovascular amyloid fibril protein. *Biochem Biophys Res Commun* 122: 1131–1135.
- Mathis CA, Wang Y, Klunk WE (2004) Imaging β -amyloid plaques and neurofibrillary tangles in the aging human brain. *Curr Pharm Des* 10: 1469–1492.
- Nordberg A (2004) PET imaging of amyloid in Alzheimer's disease. *Lancet Neurol* 3: 519–527.
- Ono M (2009) Development of positron-emission tomography/single-photon emission computed tomography imaging probes for in vivo detection of β -amyloid plaques in Alzheimer's brains. *Chem Pharm Bull (Tokyo)* 57: 1029–1039.
- Ono M, Saji H (2011) SPECT imaging agents for detecting cerebral β -amyloid plaques. *Int J Mol Imaging* doi: 10.1155/2011/543267.
- Ono M, Saji H (2012) Molecular approaches to the treatment, prophylaxis, and diagnosis of Alzheimer's disease: novel PET/SPECT imaging probes for diagnosis of Alzheimer's disease. *J Pharmacol Sci* 118: 338–344.
- Mathis CA, Wang Y, Holt DP, Huang GF, Debnath ML, et al. (2003) Synthesis and evaluation of 11 C-labeled 6-substituted 2-arylbenzothiazoles as amyloid imaging agents. *J Med Chem* 46: 2740–2754.
- Klunk WE, Engler H, Nordberg A, Wang YB, G., Holt DP, et al. (2004) Imaging brain amyloid in Alzheimer's disease with Pittsburgh compound-B. *Ann Neurol* 55: 306–319.

13. Koole M, Lewis DM, Buckley C, Nelissen N, Vandenbulcke M, et al. (2009) Whole-body biodistribution and radiation dosimetry of ^{18}F -GE067: a radioligand for in vivo brain amyloid imaging. *J Nucl Med* 50: 818–822.
14. Villemagne VL, Ong K, Mulligan RS, Holl G, Pejoska S, et al. (2011) Amyloid imaging with [^{18}F]florbetaben in Alzheimer disease and other dementias. *J Nucl Med* 52: 1210–1217.
15. Lin KJ, Hsu WC, Hsiao IT, Wey SP, Jin LW, et al. (2010) Whole-body biodistribution and brain PET imaging with [^{18}F]AV-45, a novel amyloid imaging agent—a pilot study. *Nucl Med Biol* 37: 497–508.
16. Choi SR, Golding G, Zhuang ZP, Zhang W, Lim N, et al. (2009) Preclinical properties of ^{18}F -AV-45: a PET agent for A β plaques in the brain. *J Nucl Med* 50: 1887–1894.
17. Poinsel G, Dhilly M, Moustié O, Delamare J, Abbas A, et al. (2012) PET imaging with [^{18}F]AV-45 in an APP/PS1–21 murine model of amyloid plaque deposition. *Neurobiol Aging* 33: 2561–2571.
18. Cselényi Z, Jönhagen ME, Forsberg A, Halldin C, Julin P, et al. (2012) Clinical validation of ^{18}F -AZD4694, an amyloid- β -specific PET radioligand. *J Nucl Med* 53: 415–424.
19. Kung MP, Hou C, Zhuang ZP, Zhang B, Skovronsky D, et al. (2002) IMPY: an improved thioflavin-T derivative for in vivo labeling of β -amyloid plaques. *Brain Res* 956: 202–210.
20. Kung MP, Hou C, Zhuang ZP, Cross AJ, Maier DL, et al. (2004) Characterization of IMPY as a potential imaging agent for β -amyloid plaques in double transgenic PSAPP mice. *Eur J Nucl Med Mol Imaging* 31: 1136–1145.
21. Newberg AB, Wintering NA, Plössl K, Hochold J, Stabin MG, et al. (2006) Safety, biodistribution, and dosimetry of ^{123}I -IMPY: a novel amyloid plaque-imaging agent for the diagnosis of Alzheimer's disease. *J Nucl Med* 47: 748–754.
22. Cheng Y, Ono M, Kimura H, Kagawa S, Nishii R, et al. (2010) Fluorinated benzofuran derivatives for PET imaging of β -amyloid plaques in Alzheimer's disease brains. *ACS Med Chem Lett* 1: 321–325.
23. Cheng Y, Ono M, Kimura H, Kagawa S, Nishii R, et al. (2010) A novel ^{18}F -labeled pyridyl benzofuran derivative for imaging of β -amyloid plaques in Alzheimer's brains. *Bioorg Med Chem Lett* 20: 6141–6144.
24. Ono M, Cheng Y, Kimura H, Cui M, Kagawa S, et al. (2011) Novel ^{18}F -labeled benzofuran derivatives with improved properties for positron emission tomography (PET) imaging of β -amyloid plaques in Alzheimer's brains. *J Med Chem* 54: 2971–2979.
25. Cheng Y OM, Kimura H, Ueda M, Saji H (2012) Technetium-99m labeled pyridyl benzofuran derivatives as single photon emission computed tomography imaging probes for β -amyloid plaques in Alzheimer's brains. *J Med Chem* 55: 2279–2286.
26. Cheng Y, Prusoff WH (1973) Relationship between the inhibition constant (K_I) and the concentration of inhibitor which causes 50 per cent inhibition (I₅₀) of an enzymatic reaction. *Biochem Pharmacol* 22: 3099–3108.
27. Miyaura N, Yamada K, Suzuki A (1979) A new stereospecific crosscoupling by the palladium-catalyzed reaction of 1-alkenylboranes with 1-alkenyl or 1-alkynyl halides. *Tetrahedron Lett* 36: 3437–3440.
28. Ono M, Haratake M, Saji H, Nakayama M (2008) Development of novel β -amyloid probes based on 3,5-diphenyl-1,2,4-oxadiazole. *Bioorg Med Chem Lett* 16: 6867–6872.
29. Snellman A RJ, Lopez-Picon FR, Eskola O, Wilson I, Farrar G, et al. (2012) Pharmacokinetics of [^{18}F]flutemetamol in wild-type rodents and its binding to β -amyloid deposits in a mouse model of Alzheimer's disease. *Eur J Nucl Med Mol Imaging* 39: 1784–1795.
30. Ono M, Kung MP, Hou C, Kung HF (2002) Benzofuran derivatives as A β -aggregate-specific imaging agents for Alzheimer's disease. *Nucl Med Biol* 29: 633–642.
31. Zhang W, Kung MP, Oya S, Hou C, Kung HF (2007) ^{18}F -labeled styrylpyridines as PET agents for amyloid plaque imaging. *Nucl Med Biol* 34: 89–97.
32. Hsiao K, Chapman P, Nilsen S, Eckman C, Harigaya Y, et al. (1996) Correlative memory deficits, A β elevation, and amyloid plaques in transgenic mice. *Science* 274.
33. Toyama H, Ye D, Ichise M, Liow JS, Cai L, et al. (2005) PET imaging of brain with the β -amyloid probe, [^{11}C]6-OH-BTA-1, in a transgenic mouse model of Alzheimer's disease. *Eur J Nucl Med Mol Imaging* 32: 593–600.